

## **Damping Properties of Polymer-Modified Concrete**

Hal Amick  
Colin Gordon & Associates

### **ABSTRACT**

The paper presents selected results from a broad study undertaken to explore means by which one might increase damping in concrete, which is relatively low—except for when the concrete is relatively young—and relatively independent of temperature and frequency. The most easily implemented approach involves the addition of latex admixtures to the concrete, resulting in a product generically known as polymer-modified concrete (PMC). The resulting concrete takes on some of the characteristics of the polymer involved: damping and elastic moduli become temperature and frequency dependent, and damping performance is a function of the polymer's glass transition temperature.

### **INTRODUCTION**

Concrete is an extremely popular structural material due to its low cost and easy fabrication. However, it has low damping and many engineering applications would be enhanced if the concrete technologist could design concrete mixtures with increased damping. The development of such improved concrete has received much impetus because of challenges presented in the design of facilities engaged in research and fabrication at the nanometer scale [1, 2].

This paper summarizes a portion of the results of a research project examining means by which the damping properties of concrete might be modified as part of the structural design process. The most efficacious means to achieve this objective appears to be through the introduction of latex polymers at the time of mixing. Several polymers were examined in the course of this study.

Experimental modal analysis (EMA) was used to measure modal damping and resonance frequencies in beams of rectangular cross section, supported in wire slings, and excited in free-free modes. By using multiple bending modes, data were obtained over a frequency range between about 150 Hz and 3000 Hz. The specimens were tested at several temperatures, and the loss factor and elastic moduli were found to be dependent upon both frequency and temperature.

The method of reduced variables was used to combine the effects of frequency and temperature, leading to the observation that polymer-modified concrete exhibited behavior similar to polymers. It is feasible to use polymer additives to significantly enhance concrete's damping but, as with polymers used for applications such as constrained layer damping, the designer must give consideration to the ambient temperature and the frequency range of concern.

### **MATERIALS EXAMINED**

The coarse and fine aggregates (e.g., gravel and sand), as well as the ASTM Type III portland cement, were commercially available bagged products. The coarse aggregate had 10 mm (3/8 in.) maximum size aggregate.

Many polymers—particularly those characterized as “viscoelastic”—are known to possess desirable damping properties. Many of these are well documented, and a variety of methods exist in which viscoelastic polymers may be incorporated into plate and beam components of several types of structures [3].

Viscoelastic polymers may be incorporated into concrete in a number of ways. (Some polymer treatments of concrete involve polymers that are not traditionally considered “damping materials,” including epoxy, though the resulting concrete will take on some of the damping properties of the polymer. However, these mix designs, many of which do not involve portland cement, not included in this study.) Prior studies have examined effects on damping when using asphalt-coated aggregate [4], ground rubber from tires [5], and other forms of latex [6, 7]. In each case, the studies were limited to observations that damping increased with the concentration of the polymer. None of these studies examined the role of temperature and frequency.

A number of polymer admixtures were used in the study. The dynamic properties of concrete with these admixtures had not been examined previously. Three were liquid latex suspensions of styrene-butadiene rubber (SBR) in water. Some of the properties are given in Table 1, including the glass transition temperatures,  $T_g$  [8]. SBR-A is popular for use in concrete pavements, in part because of its improvement of durability. The other two are not used extensively. The specific gravity of these admixtures is approximately 1.02.

Table 1. Styrene-butadiene rubber (SBR) latex suspensions used in the study; S/B,  $T_g$ , and Percent Solids from Barclay (2004) [8]

Designator	S/B	$T_g$ (°C)	Percent Solids	pH
SBR-A	60/40	10	48%	9.0
SBR-447	55/45	-17	47.5%	10.3
SBR-813	40/60	-41	47%	10.1

Table 2. Summary of compressive strengths at ~28 days

Polymer	W/C	P/C	$f_c'$ , MPa
none	0.53		33.0
SBR-A	0.2	0.2	39.0
SBR-447	0.2	0.2	32.5
SBR-813	0.2	0.2	26.7
EVA	0.42	0.2	18.7
SBR/g	0.63	0.03	18.6

determinant of concrete strength. The term P/C represents the weight ratio of polymer solids to cement. Shown are the upper-bound P/C values used for all experiments except those in which concentration was varied.

A fourth polymer additive included in the study was ethyl-vinyl-acetate (EVA) powder, popular as an additive to commercially prepackaged tile grout. It has a  $T_g$  of 11.2°C [9]. In this study, it was mixed with the dry cement prior to mixing.

The fifth polymer additive is an emulsion of vegetable gum suspended in SBR-A liquid latex suspension and denoted herein as SBR/g. The gum results from soybean oil reacted with sulfur monochloride. The gum and latex components are mixed at a gum:latex ratio of 6:44. The resulting latex has a specific gravity of 1.036 and a pH of 0.9, and it consists of 48% polymer solids.

The important concrete mix parameters, including concrete compressive strength, are summarized in Table 2. The term W/C represents the weight ratio of water to cement solids, the primary

### TEST CONFIGURATION

EMA was performed on beams of rectangular cross section, 89 mm x 114 mm (3.5 in. x 4.5 in.), with a length of 1400 mm (55 in.). They were supported in wire slings and tapped with a small modal hammer having a mass of 235 g. A 100mV/g accelerometer, attached using a threaded stud to mounts cast in the concrete, was used as a vibration sensor. Figure 1 shows the measurement locations. Locations 2 and 3 were excited in the orientation shown; the specimens were rotated 90° (such that axis 2 was horizontal) for excitation of Location 1. Bending about axis 1 and axis 2 were denoted by B1 and B2, respectively. Signal processing was carried out using a commercial laptop-based two-channel spectrum analyzer, and commercial modal analysis software was used to extract frequencies and modal damping from acceleration FRF spectra using curve fitting.

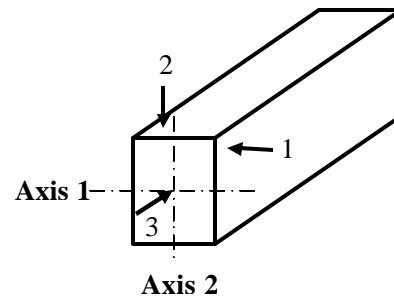


Figure 1. Schematic diagram of excitation and measurement locations: (1) bending about axis 1 and torsion; (2) bending about axis 2 and torsion; (3) longitudinal. Specimen was rotated 90° for axis 2 measurements.

The fundamental bending resonance frequencies of this beam configuration—with unmodified concrete—were about 210 Hz and 165 Hz for B1 and B2, respectively. The longitudinal fundamental frequency was about 1100 Hz. By using multiple bending modes, data were obtained over a frequency range from about 150 Hz to about 3000 Hz.

The sling provided three pendulum modes with respect to the specimen: two lateral modes and rotation about the vertical axis. The frequencies associated with these modes were 0.32, 0.31, and 0.44 Hz, respectively, or periods of 3.1, 3.2 and 2.3 sec. The support frequencies are significantly less than those of the beams, so the modes are well decoupled.

### CALCULATING MODULUS FROM MEASURED RESONANCE FREQUENCY

If one is able to directly measure the mass of a beam with known geometric properties, and experimentally determine its resonance frequencies, then the well-known expression [10] relating frequency to material and geometric properties may be rearranged such that Young’s modulus  $E_i$  for the  $i^{\text{th}}$  mode may be calculated

$$E_i = \frac{4m\mathbf{p}^2L^3}{II_i^4} f_i^2, i = 1, 2, 3 \dots \quad (1)$$

in which  $L$  is the beam’s length,  $I$  is the beam’s area moment of inertia, and  $m$  is its mass per unit length. This approach neglects the effects of rotational inertia, and presumes a long, slender, prismatic beam. The parameter  $l_i$  depends upon support conditions. Blevins [10] has tabulated values of  $l_i$  for many modes and support conditions; the first three for a free-free beam are approximately 4.73, 7.85, and 10.99. Similar equations exist for torsional and longitudinal deformation [10].

The shorter specimens clearly cannot be characterized as long and slender beams, and the longer specimens are not slender with respect to the higher modes. Finite element models were constructed of the two beam configurations using 3-D “brick” elements and typical properties for plain concrete. It is possible to calculate the approximate elastic modulus  $E(f_i)$  for the  $i^{\text{th}}$  mode using

$$E(f_i) = \frac{E_0mf_i^2}{m_0f_0^2} \quad (2)$$

in which  $f_i$  is the measured bending frequency for mode  $i$ ,  $m$  is the measured mass of the beam, and  $E_0$ ,  $m_0$ , and  $f_0$  are the corresponding quantities used in the finite element analysis. Likewise, the shear modulus  $G_i$  may be estimated from the measured torsional frequency and the calculated torsional frequency from the finite element model.

### MEASURED RESULTS

A preliminary study was carried out using shorter specimens with a length of 406mm (16 in.) in order to document the effect of polymer concentration when using SBR-A, EVA and SBR/g, using three specimens of each mix. It is customary to represent polymer concentration in PMC by means of the ratio of the weight of polymer solids to that of the dry cement, a quantity commonly denoted P/C. The tests were performed at an age of about 4 weeks. The loss factors for fundamental modes of B1 and B2, torsion and extensional deformation were averaged together. The results are shown in Figure 2, which shows the effect of varying P/C for three polymers with  $T_g$  near room temperature, SBR-A, SBR/g, and EVA. Each of these polymers exhibits a nearly linear relationship between P/C and loss factor.

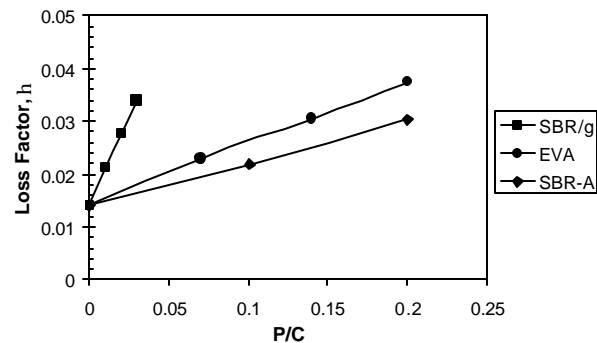


Figure 2. Effect of polymer concentration, P/C, on average loss factor at room temperature and  $1450 = f = 4200$  Hz, room temperature, age between 4 and 5 weeks.

The damping in these three polymers may be represented by a simple relationship

$$h = h_0 + a \frac{P}{C} \quad (3)$$

in which  $h_0$  represents the damping of concrete without the polymer and  $a$ , the slope in the equation, represents the polymer's effectiveness at damping enhancement.

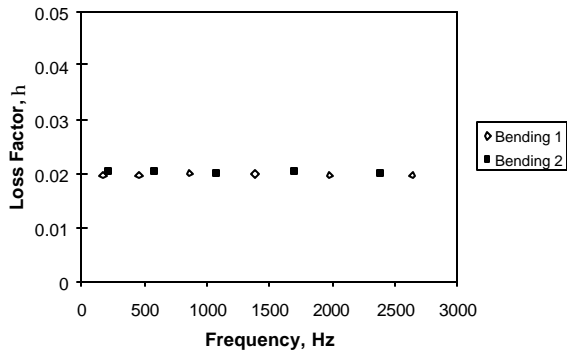


Figure 3. Modal damping of long rectangular beam of plain concrete.

Modal tests were performed on one of the longer beams fabricated from plain concrete (concrete without a polymer additive) to provide a basis of reference for the tests with PMC. The results of these tests demonstrated that loss factor remained constant with frequency, as shown in Figure 3.

Polymers by themselves are known to exhibit different frequency-dependent loss factor curves depending upon temperature. The set of long PMC specimens was subjected to several ambient temperatures, ranging from -3°C to 27°C. (All of these specimens were of the maximum P/C shown in Figure 2.) The specimens were stored overnight at the desired temperature, and tested the following morning after the temperature distribution had stabilized. The modal tests were performed in a lab at room

temperature, but the test protocol allowed the entire test sequence to take less than ten minutes, during which time there was very little change in temperature over the beam cross section.

Figure 4 shows the damping measured for bending in the weak (B1) direction in the beam modified with SBR-A ( $T_g = 10^\circ\text{C}$ ). Figure 5 shows the corresponding data for SBR-447 ( $T_g = -17^\circ\text{C}$ ). The maximum loss factor measured for both SBR-A and SBR-447 was 0.038 at 27°C and -3°C, respectively, between 500 and 1000 Hz. Note that the loss factor for SBR-A generally *increases* with temperature, while that of SBR-447 *decreases* with increasing temperature.

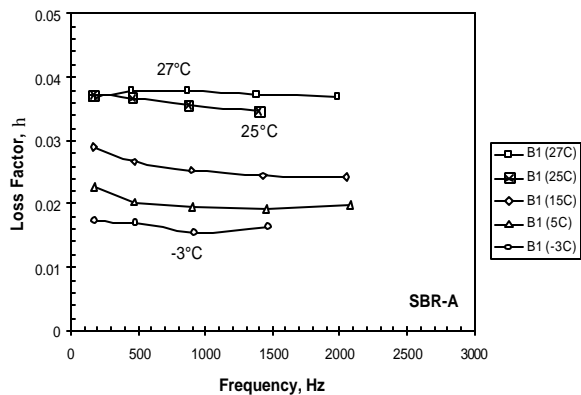


Figure 4. Loss factor at five temperatures in LR beam modified SBR-A ( $T_g = 10^\circ\text{C}$ ).

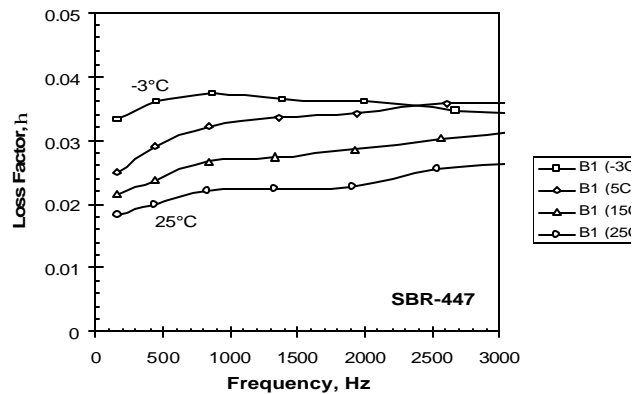


Figure 5. Loss factor at four temperatures in LR beam modified with SBR-447 ( $T_g = -17^\circ\text{C}$ ), organized by ambient temperature.

### SHIFTING BY FREQUENCY

The loss factors for B1 modes of PMC with SBR-A shown in Figure 3 may be combined with those of the B2 modes and, together with the Young's moduli for B1 and B2 modes, may be used to manually shift data as a function of frequency in the classical WLF method [11] of reduced variables as presented by Ferry [12]. The shifted data are

shown in the top part of Figure 6. The temperature shift factors, shown in the bottom part, were selected such that  $a_T = 1$  at 25°C. The loss modulus—the product of Young’s modulus and loss factor—is also shown as open symbols. A similar process for SBR-447 will lead to the results shown in Figure 7.

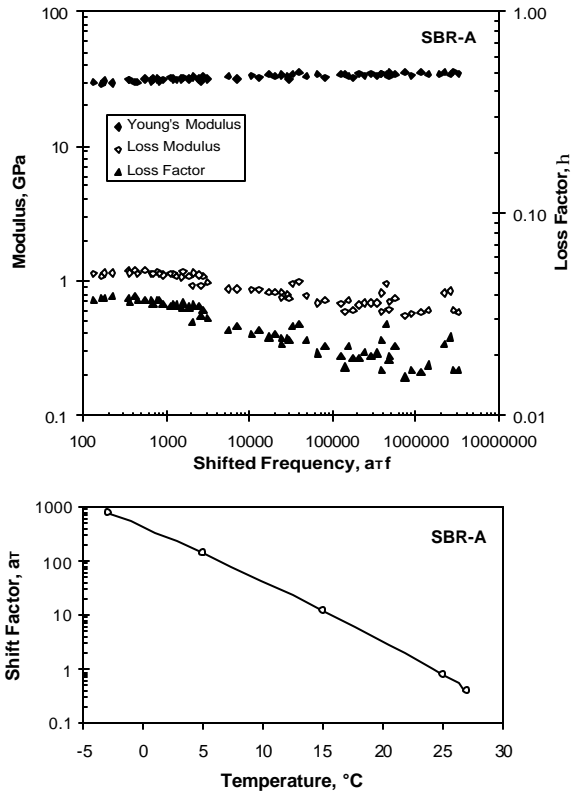


Figure 6. Data for beam modified with SBR-A ( $T_g = 10^\circ\text{C}$ ), shifted by frequency using the protocol of reduced variables, showing loss factor (top) over an extended frequency range, and shift factor (bottom), with  $a_T = 1.0$  at  $25^\circ\text{C}$ .

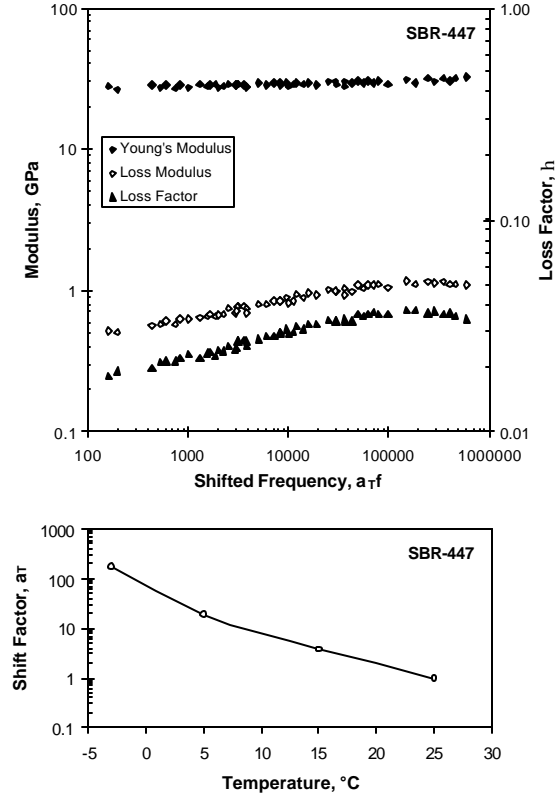


Figure 7. Data for beam modified with SBR-447 ( $T_g = -17^\circ\text{C}$ ), shifted by frequency using the protocol of reduced variables, showing loss factor (top) over an extended frequency range, and shift factor (bottom), with  $a_T = 1.0$  at  $25^\circ\text{C}$ .

It may be seen that over this range of temperatures and frequencies, the concrete with SBR-A (Figure 6) exhibits the peak loss factor and a portion of the right side of a family of curves similar in shape to those appropriate for SBR in general [2]. The concrete with SBR-447 (Figure 7) shows the peak loss factor and the left side of those characteristic curves. These observations suggest that over a much larger temperature range enclosing both glass transition temperatures, there would be the full set of curves similar to those for SBR.

However, it is important to note the limited range of loss factor and modulus in these figures. SBR normally exhibits a loss factor range of almost an order of magnitude, and a range of Young’s modulus of several orders of magnitude. In PMC the loss factor varied only about 30%, but the Young’s modulus varied even less, about 12%.

The data in Figure 5 may be rearranged by mode, rather than by temperature, and plotted as functions of temperature, as shown in Figure 8. A peak in the data is evident at approximately 5°C for the Mode 6 and 7 curves. The curves may be shifted left and right by frequency such that the data all fall along a single curve, as shown in Figure 9. The temperature shifts  $\Delta T$  required to achieve this alignment are plotted as a function of frequency in Figure 10. (For simplicity, the frequencies associated with each shift are taken as the averages of the frequencies associated with each mode. A slight error is introduced by this simplification.) The shift is a linear function of the log of frequency. The concrete from the other polymer formulations exhibited similar behavior.

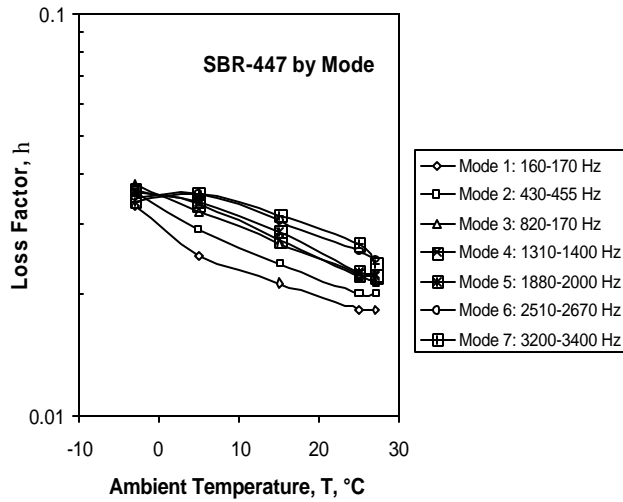


Figure 8. Loss factor at four temperatures in beam modified with SBR-447 ( $T_g = -17^\circ\text{C}$ ), organized by B1 bending mode number.

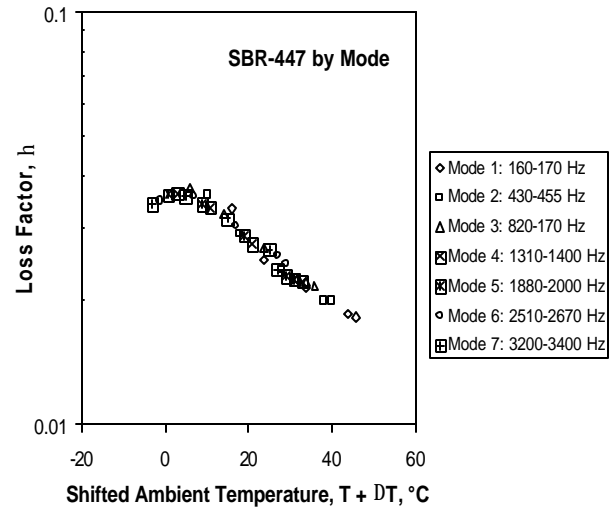


Figure 9. Loss factor as a function of shifted temperature, by B1 mode, for LR beam modified with SBR-447 ( $T_g = -17^\circ\text{C}$ ).

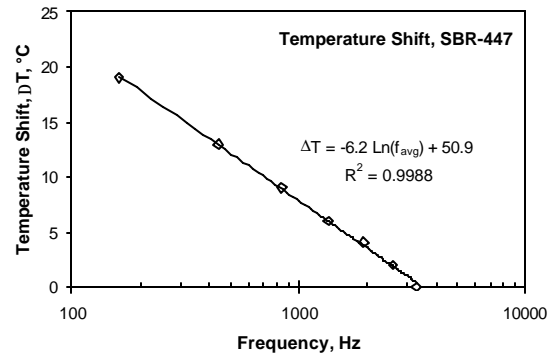


Figure 10. Temperature shift factor required to convert data from the format of Figure 9 to that of Figure 10, for B1 mode in beam modified with SBR-447 ( $T_g = -17^\circ\text{C}$ ).

The individual loss factor data points from the reduced variables plots may be smoothed such that they may be represented by curves. These smoothed curves are compared in Figure 11. Upon examination of only the curves for SBR-A and SBR-447, we see two halves of a possible characteristic shape for SBR in general. However, without actually testing the SBR-A beams at lower frequency (or higher temperature) and the SBR-447 beams at higher frequency (or lower temperature) it is impossible to confirm if the “master curves” can simply be shifted by some function of  $T_g$ , or if the shapes are unique. Although the curves appear to be reaching constant values at their minima, this aspect is also impossible to confirm without extending the frequency or temperature range.

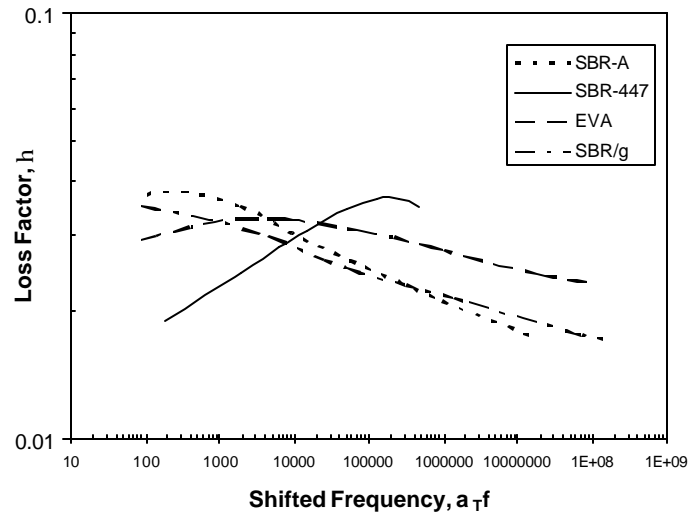


Figure 11. Shifted loss factors beams modified with SBR-A, SBR-447, SBR/g, and EVA, with  $a_T = 1.0$  at 25°C.

### GENERALIZATIONS

The data suggest that the maximum damping available in PMC is related to both polymer concentration and the glass transition temperature  $T_g$  of the particular polymer. It appears that in the frequency range of interest to structural dynamicists and acousticians dealing with structureborne noise in conventional structures, the maximum damping occurs when  $T_g$  is at or slightly below the ambient temperature. Increasing  $T_g$  also increases the temperature at which peak damping occurs.

Within the range examined in this study, damping varies linearly with polymer concentration. This means that the shapes of the curves in Figure 11 must also vary with concentration. The effect of concentration on the frequency distribution of loss factor is suggested in Figure 12. As concentration approaches zero, the curve flattens and approaches that of plain concrete. Modulus curves are not shown in Figure 12 because the experimental data from the present study are not complete enough to clarify what happens to modulus as the concentration approaches zero.

If ambient temperature is changed, the loss factor and modulus curves shift horizontally, as shown in Figure 13. Increasing the ambient temperature shifts the peak to the left, such that the peak occurs at lower frequencies. The modulus curves also shift to the left, but since the variation with frequency is already small, the modulus change due to temperature shift is virtually negligible.

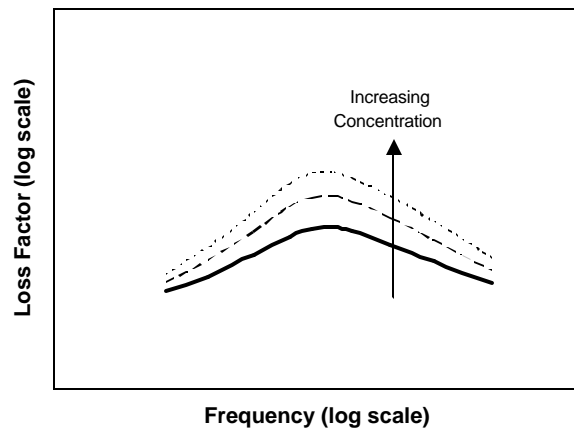


Figure 12. Typical curves showing effect of frequency on loss factor of polymer modified concrete as polymer concentration is varied.

It is important to note that the simple shifts shown in Figure 13 are, in practice, most likely bounded. At temperatures well below 0°C, the entrained free water tends to freeze and ice crystals begin to form in the pore spaces. This may affect damping properties of the concrete (though this is unproven). However, the change in dynamic properties of the polymers probably conforms to the behavior of the polymer alone. At temperatures well above 100°C, the entrained water can vaporize, which may also change the concrete's properties. Neither of these extrema was examined in the present study.

Furthermore, the inverse relationship between temperature and frequency suggests that the shift to the right on a  $\eta$ -T graph as  $T_g$  increases would correspond to a shift to the left on a  $\eta$ -f graph. This is illustrated in Figure 14. Thus, if maximum damping is desired at extremely low frequencies (as associated with lateral building vibrations), a  $T_g$  or 10°C or lower should be used. On the other hand, if maximum performance is desired at higher audible frequencies (say, a few thousand hertz), then a higher  $T_g$  should be used.

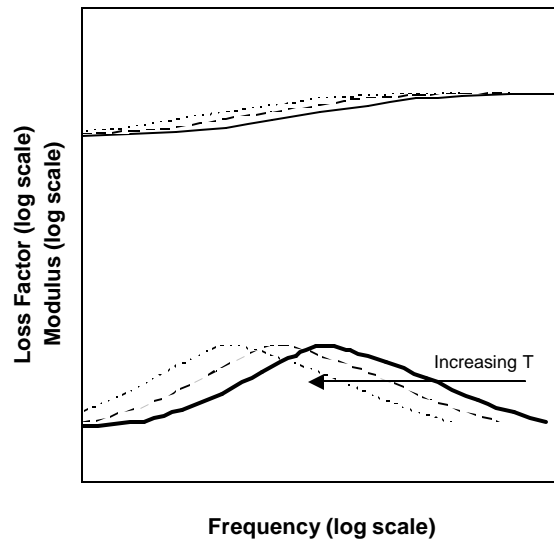


Figure 13. Typical curves showing effect of frequency on loss factor and modulus at several ambient temperatures.

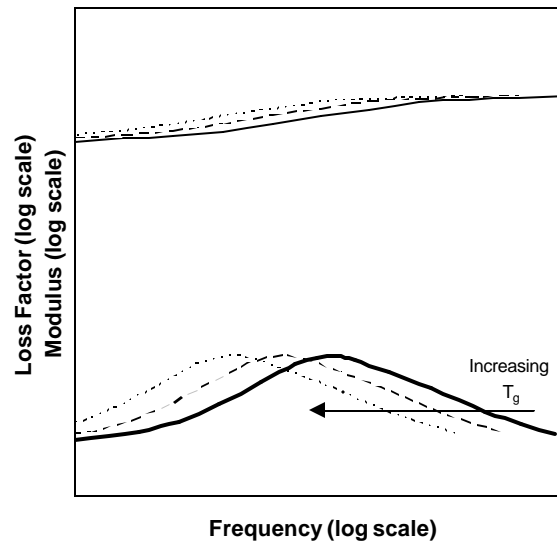


Figure 14. Typical curves showing effect of frequency on loss factor and modulus at several glass transition temperatures.

## CONCLUSIONS

The experimental data suggest that the introduction of polymers to concrete in the form of latex additives results in a blending of the material properties, such that the dynamic properties of the resulting PMC exhibit characteristics of each component. The moduli and loss factor become dependent on frequency and temperature, unlike those of concrete alone. The range of loss factor is significantly reduced, but remains variable enough that it should be taken into



consideration by a designer. The ranges of Young's and shear moduli are reduced enough that for all practical purposes they may be considered constant.

The present study demonstrated a linear relationship between loss factor and polymer concentration, and that latex admixtures could more than double the loss factor of plain concrete. This would reduce by more than half the resonance amplification provided by a concrete structure. The concentration was kept to within arbitrary limits for this study, and it appears that further increases of damping are possible.

Although unreported in this paper, it should be noted that polymer modification also has an impact on strength (generally a reduction), durability (generally an improvement) and fire resistance (it may combust), all features of concern to a structural engineer.

### ACKNOWLEDGEMENTS

The author wishes to acknowledge the financial support of Walter Israel and Durasol Corporation, assistance provided in the lab and at the mixer by graduate student Cruz Carlos Jr., and the technical feedback and guidance provided by Paulo Monteiro, Ahid Nashif, Denise Silva, and Eric E. Ungar.

### REFERENCES

1. Amick, H., Sennewald, B., Pardue, N. C., Teague, C., and Scace, B. (1998), "Analytical / Experimental Study of Vibration of a Room-Sized Airspring-Supported Slab," *Noise Control Engineering Journal*, March/April 1998, v. 46, no. 2, pp. 39-47.
2. H. Amick, H., and Monteiro, P. J. M., "Vibration Control Using Large Pneumatic Isolation Systems with Damped Concrete Inertia Masses," *Proc. 7<sup>th</sup> Intl. Conf. on Motion and Vibration Control, (MoViC 04)*, Paper 118, August 8-11, 2004, Washington University, St. Louis, MO.
3. Nashif, A. D, Jones, D. I. G., and Henderson, J. P. (1985), *Vibration Damping*, John Wiley and Sons, New York, 453 pp.
4. Mayama, M. (1987), "Vibrating properties of coated ferrite concrete," *Proceedings, Japan Society of Civil Engineers* (Tokyo), No. 384, July 1987, pp. 93-101.
5. Kerševicius, V., and Skripkiunas, G. (2002). "Physical Properties and Durability of Concrete with Elastic Additive from Rubber Waste," *Materials Science (Medžiagotyra; ISSN 1392-1320)*. Vol. 8, No. 3. 2002, pp. 293-298.
6. Ohama, Y. (1995), *Handbook of Polymer-Modified Concrete and Mortars*, Noyes Publications, 236 pp.
7. Wong, W.G., Fang, P., and Pan, J.K. (2003), "Dynamic properties, impact toughness and abrasiveness of polymer-modified pastes by using nondestructive tests," *Cement and Concrete Research*, Vol. 33, No. 9, pp. 1371–1374.
8. Barclay, D. (2004), personal communications via emails to Hal Amick dated 1/19/2004 and 1/23/2004.
9. Silva, D. (2003), Private communication.
10. Blevins, Robert D. (1979), *Formulas for Natural Frequency and Mode Shape*, Kreiger Publishing Co., 1979, 492 pp.
11. Williams, M. L., Landell, R. F., and Ferry, J. D. (1955), "The Temperature Dependence of Relaxation Mechanisms in Amorphous Polymers and other Glass-forming Liquids," *Journal of the American Chemical Society*, Vol. 77, No. 14, pp. 3701-3706.
12. Ferry, J. D. (1961), *Viscoelastic Properties of Polymers*, John Wiley and Sons, New York, 482 pp.